

Estimation of Attrition Loss Due to Spray-On Coatings for Mg Alloys Using a Novel Machine Learning Approach

Alka Singh¹, Dr. Trapy Agarwal², Dr. Vinima Gambhir³, Adarsha Harinaiha⁴

¹*Assistant Professor, Master of Computer Applications, Noida Institute of Engineering and Technology, Greater Noida, Uttar Pradesh, India, Email Id- alka@niet.co.in*

²*Associate Professor, Maharishi School of Engineering & Technology, Maharishi University of Information Technology, Uttar Pradesh, India, Email Id- trapy@muit.in*

³*Associate Professor, Department of ISME, ATLAS SkillTech University, Mumbai, Maharashtra, India, Email Id- vinima.gambhir@atlasuniversity.edu.in*

⁴*Professor, Department of Mechanical Engineering, Faculty of Engineering and Technology, JAIN (Deemed-to-be University), Ramanagara District, Karnataka - 562112, India, Email Id- h.adarsha@jainuniversity.ac.in*

Protective coatings are essential for improving magnesium (Mg) alloy performance and longevity in a variety of industrial environments. The wear and tear, or attrition loss, that these coatings endure over time, continues to be a major problem. Conventional techniques to calculate attrition loss are imprecise and unable to consider the intricate relationships between coating components and surroundings. Our research suggests a novel machine learning (ML) method to forecast attrition loss in magnesium alloys with spray-on coatings as a solution to this problem. For the forecasting model in this paper, adaptive seagull optimization integrated random forest (ASO-RF) strategy is suggested. Wear loss data that was actually obtained for AZ91D Mg-alloyed specimens that were sprayed with various settings was used in this investigation. With the help of the gathered dataset, the ASO-RF algorithm is trained, allowing for precise attrition loss forecasts under different circumstances. In terms of attribute loss prediction, the suggested ASO-RF method's performance in Matlab implementation is examined and contrasted. This method presents a viable way to maximize coating formulas and thicknesses to reduce attrition, improving the overall performance and durability of magnesium alloys.

Keywords: Spray-On Coating, Industrial Environments, Mg Alloy, Attrition Loss, Machine Learning (ML), Adaptive Seagull Optimization Integrated Random Forest (ASO-RF).

1. Introduction

Magnesium (Mg) alloys have attracted a lot of interest from a variety of sectors because of

its exceptional strength-to-weight ratio, low density and amazing machinability [1]. The wear and corrosion susceptibility of magnesium alloys limits their long-term durability and performance, which makes their practical application difficult. The use of protective coatings has become a viable alternative in an attempt to overcome these obstacles [2]. Spray-on coatings have attracted attention due to their adaptability, simplicity of use and capacity to offer a consistent layer of protection on magnesium alloys [3]. By acting as a barrier, these coatings protect the underlying alloy from abrasive and corrosive environments [4]. Even though these coatings have clear advantages, it's critical to recognize and estimate any potential attrition losses that can happen in the future [5].

Attrition loss describes the slow deterioration and wear of the protective layer under service circumstances in the context of spray-on coatings for magnesium alloys [6]. Numerous variables, such as the coating material's intrinsic qualities, mechanical loads and environmental exposure, might have an impact on this occurrence [7]. Determining the lifespan of coated magnesium alloys and refining coating formulas for improved performance need a precise prediction of attrition loss [8].

Estimating attrition loss for magnesium alloys with spray-on coatings presents a substantial potential as businesses increasingly use machine learning technologies for predictive analysis and optimization [9]. The empirical models used by traditional attrition loss prediction approaches cannot be as detailed or flexible as needed to account for the intricate interactions between variables that affect coating wear over time [10]. Attrition loss for spray-on coatings on Mg alloys includes potential uneven coating distribution, difficulty in establishing uniform thickness and challenges in sustaining adhesion under harsh temperatures. Furthermore, differences in coating qualities can impair long-term durability, needing careful consideration for practical applications [11].

Study [12] obtained the experimentation on abrasive deterioration for AZ91D alloy of magnesium samples covered with two different spraying coating techniques with different parameters. The extreme learn machine (ELM) and support vector regression (SVR) techniques were used to forecast wear degradation values. The SVR approach was beaten by the ELM approach. Because of this, the ELM technique has a great chance of helping with the spray coating process to fabricate durable components for a range of applications. Study [13] investigated the influence of wear factors on the wear rate (WR) of magnesium (AZ91) composites. Artificial neural networks (ANN), adaptable neuro-fuzzy inference algorithms (ANFIA) and decision tree structures (DT) are examples of methods from machine learning (ML) that were used to build an efficient model for prediction for predicting the outcomes at the appropriate input parameters. When compared to other models evaluated in their study, the DT model was found to be more accurate.

Study [14] explored ZrO_2 -wt.-% 22 MgO was laser blasted over the outermost layer of an AZ91D mg alloy. The roughness of the surface was assessed using a profilometer and toughness was determined using the micro-hardness test. The identified portions that were addressed using an optics microscope (OM) and scanning electron microscopy (SEM). One of the ML methods, the ELM algorithm, was applied to utilize damaged data. The model developed using the ELM approach had an R-squared coefficient success rate. Study [15] provided the effects of incorporating Mg into ZA-27 alloy on both its characteristics of

morphology and tribology. There was variation in the Mg concentration. We evaluated proportional rate of wear for a range of operational conditions. Aspect detection and surface inspection were achieved by using SEM and X-ray diffraction (XRD) methods. The experiment finding demonstrate that the Mg concentration of 0.5% exhibited the lowest wear rate.

Study [16] provided the rate of degradation (WD) of ZnO-filled AA7075 composite was examined using the data-driven decision trees (DT) technique. The Taguchi technique indicates that a 10% reinforcement content, an applied load, a sliding velocity and distance are the ideal level factors for getting the least WD. The results of the DT algorithm experiments, reinforcing was the primary component controlling the material's wear, as confirmed by the Taguchi-based technique's examination of variation and ratio of signal to noise investigation. The development and prediction of corrosion rate of magnesium alloys based on the composition of the magnesium chemical alloy as independent input variables was achieved in study [17] through the use of various training algorithms, including K-nearest neighbor (KNN), artificial neural network (ANN), decision tree (DT), extra tree (ET), random forest (RF) and linear regression (LR). The result indicates that among ML and RF algorithm has the biggest impact on predictions.

Study [18] demonstrated the track and categorizes sliding bearings' multi-variant wear behaviour. The acoustic emission (AE) approach was utilized on a sliding bearing test setup to achieve this goal. A hydrodynamic bearing operation's irregularities were identified by evaluating AE signals using machine learning techniques. The classification accuracy was compromised due to the potential misinterpretation of the incubation period at the commencement of inadequate lubrication as running-in and vice versa, in certain cases. Study [19] provided the machine learning techniques, such as extreme gradient boosting (XGB) and ANNs, to calculate the bidirectional fiber-reinforced polymeric compound's degradation rate and to compare the performance of the various algorithms. The most important characteristics of the input, according to the XGB model, are contact particles acceleration, contact position and the orientation of the fibers.

Study [20] developed a wear resistant mass reduction forecasting technique for sporting goods utilizing the highest probability estimate for durability assessment. The results demonstrate their method's low wear and strong wear resistance, as well as its steady increase in coating mass loss with increasing load. Sports gear coated with this technique has wear absorbed approximately.

The purpose of this study is to improve the general efficiency and long-term reliability of magnesium alloys in various industrial environments by addressing the enduring problem of inaccurate attrition loss estimation in magnesium oxide alloys with protective paints and offering a useful tool for optimizing covering mixes and levels of thickness.

The remaining portion of this article is as follows: Part 2 discusses the methodology. In Part 3 of this article, we provide the result and discussion. The concluding segment of this article, Part 4, summarizes the key findings and contributions of our research.

2. METHODOLOGY

2.1 Data collection

The samples of AZ91D magnesium alloy measuring 20 mm in diameter and 50 mm in length were employed as substrates. Materials were immersed in an ultrasonic bath for fifteen minutes after being cleaned with ethanol to remove oil and debris from their exterior surfaces. They were humidified with hot air and washed with distilled water before that is placed in an ultrasonic bath for a further fifteen-minute period. The parts of the object that were intended to be covered were modified to improve coating absorption and sanded using Al_2O_3 sand at a pressure of five bar and chemical composition shown in Table 1.

Table 1. The AZ91D magnesium alloy's chemical composition (Source: Author)

Alloy	Composition
Al	8.6-9.6
Cu	0.026 max
Mg	89-91.51
Mn	0.18-0.5
Si	0.051 max
Zn	0.46-0.10
Other metals	Rest

To enhance coating adherence, the surfaces that were going to be covered were roughened and sanded using Al_2O_3 mud pressurized of 5 bar. Table 2 displays the attributes of the ZrO_2 -wt % 22Mgo coating powder was applied using plasma spraying. Table 3 displays the features of the HVOF-powdered satellite-1, GTV trademark.

Table 2. Properties of ZrO_2 -Mgo coated powder (Source: Author)

Ceramic	Particle size	Chemical composition (wt. %)
ZrO_2	$-46 + 21\mu\text{m}$	79
Mgo		23

Table 3. Properties of Stellite-1 coating powder (Source: Author)

Particle size	Element	Chemical composition (wt. %)
$-54+21\mu\text{m}$	Co	Bal.
	Cr	31
	W	13
	C	1.6

The substrates were roughened and coated with ZrO_2 -wt % 22Mgo utilizing plasma spraying, as shown in Table 4. Table 5 displays the coating parameters for the HVOF process.

Table 4. Coating parameter for plasma spraying (Source: Author)

Sample number	S_1	S_2	S_3	S_4	S_5	S_6
Current (A)	601	601	601	501	501	501
Spray distance (mm)	121	131	141	121	131	141
Rate of feeding for powders (g/min)	41	-	-	-	-	-
Circulation rate of hydrogen electric gas (l/min)	11	-	-	-	-	-
The movement rate of the argon shielded gas (l/min)	36	-	-	-	-	-
Amount of voltage (V)	151	-	-	-	-	-

Table 5. Coating parameter for the HVOF process (Source: Author)

Sample number	S_7	S_8	S_9	S_{10}	S_{11}	S_{12}
Oxygen flow rate (l/min)	251	251	251	201	201	201
Propane flow rate (l/min)	61	61	61	51	51	51
Spray distance (mm)	261	271	281	261	271	281
The velocity of flow of nitro gases as carriers (l/min)	26	-	-	-	-	-

Rate of feeding for powders (g/min)	51	-	-	-	-	-
Velocity of traversal (mm/s)	101	-	-	-	-	-

2.2. Data preprocessing

Min-Max normalization:

The min-max normalization ensures that diverse variables with varying scales contribute equally to the analysis, making attrition loss data comparability easier. Normalizing input data improves model efficacy by preventing specific traits from dominating the analysis merely on the basis of their magnitude.

The original data is linearly altered by min-max normalization as shown in Equation (3). The normalized values fall within the specified range. The calculation is provided for mapping a v value of an attribute A from range $[min_A, max_A]$ to a new range $[new_min_A, new_max_A]$.

$$\frac{v - min_A}{max_A - min_A} (new_min_A, new_max_A) + new_min_A \quad (1)$$

2.3. Adaptive seagull optimization (ASO)

ASO method is its quick convergence speed, low computational cost and ability to solve large-scale constrained problems. It has a lot of advantages over other optimization algorithms. A global optimization search process of ASO is linear in equation (2).

$$A = fc - (t \times (fc / Max_{iteration})) \quad (2)$$

When the variable's value decreases from 2 to 0 and $t = 0, 1, 2, \dots, Max_{iteration}$ Max iteration, fc can regulate the frequency of the variable.

The global search capacity of SOA cannot be leveraged due to this linear search strategy. We provide a nonlinear search control formula, represented by Equation (3), which can be used to enhance the algorithm's speed and accuracy by focusing on the seagull group exploration phase stage as shown in Equation (3).

$$A = fc \times \frac{1}{e^{4 \cdot \left(\frac{t}{Max_{iteration}}\right)^{4r}}} \quad (3)$$

Where e is the natural logarithm's base.

2.4 Random forest (RF)

This algorithm is a comprehensive ensemble method that consists of several decision trees. The integrated method utilizes bagging to generate multiple independent decision trees and the final results are selected based on the average or majority voting principle. This approach is employed to mitigate the potential danger of data over-fitting. The performance of the RF model is strongly influenced by two crucial factors, namely the number of *entry* and *tree*,

throughout the forest creation process. In the conventional RF model, the selection of values for *ntree* and *mtry* is guided by empirical knowledge and it is subjected to a certain level of uncertainty.

The forest is composed of up of numerous decision trees $\{h(x, \theta_j), m=1,2,3,\dots,N\}$.

Using the bootstrap approach to generate j sets $\theta_1, 2, \dots, \theta_j$ and the accompanying j decision trees by repeating random extraction of original data.

In the case when the feature space is M -dimensional, it is necessary to determine the constant m and thereafter select m sub-feature sets randomly from the M -dimensional feature space. By following this approach, the optimal segmentation can be obtained by the establishment of the decision tree.

The growth of each decision tree occurs without the implementation of pruning techniques, allowing it to expand unrestrictedly until it reaches a point where further splitting is no longer feasible.

The process involves generating j decision trees to form a random forest ensemble. The best decision tree is determined by a voting mechanism.

The ultimate result is obtained by calculating the average value of j decision trees $h(x, \theta_j)$.

2.5. Adaptive seagull optimization integrated random forest (ASO-IRF)

The Magnesium (Mg) alloy spray-on coating attrition loss can be reduced with the innovative ASO-IRF method. This novel approach improves the performance of protective coatings by combining the advantages of Random Forest (RF) and Adaptive Seagull Optimization (ASO) algorithms.

ASO improves the coating process for magnesium alloys by adjusting its search parameters, using inspiration from the shrewd foraging habits of seagulls. This ability enables effective solution space exploration, enhancing the adhesion and robustness of the coating.

ASO-IRF uses ensemble learning to assess and forecast attrition loss patterns and it is integrated with Random Forest, a powerful machine learning method. The utilization of several decision trees in Random Forest (RF) methodology improves the precision of forecasts, enabling the determination of optimal coating parameters that offer the highest level of protection against attrition shown in algorithm 1.

Algorithm 1: Adaptive Seagull Optimization Integrated Random Forest (ASO-IRF)

```
function adaptive_seagull_optimization(objective_function, initial_solution):  
    initialize_seagulls()  
    while not convergence_criteria_met:  
        update_seagull_positions()  
        evaluate_fitness(objective_function)  
        update_seagull_parameters()
```

```

return best_solution
function random_forest(train_data, train_labels, test_data):
    initialize_forest()
    for tree in forest:
        bootstrap_sample = create_bootstrap_sample(train_data, train_labels)
        grow_tree(tree, bootstrap_sample)
    return predict_majority_vote(forest, test_data)
function aso_irf(coating_data, attrition_loss_labels):
    best_coating_params =
        adaptive_seagull_optimization(objective_function, initial_solution)
    optimized_coating_data =
        apply_coating_params(coating_data, best_coating_params)
    predicted_attrition_loss =
        random_forest(optimized_coating_data, attrition_loss_labels, test_data)
    return best_coating_params, predicted_attrition_loss \

```

3. RESULT AND DISCUSSION

We used three distinct assessment standards R-square (R^2), mean absolute error (MAE) and root mean square error (RMSE) to evaluate the existing method ANN, ELM [21] and proposed method ASO-RF. We applied HVOF and plasma spray-coated magnesium alloys to data collected from dry slide wearing trials. 220 experimental data points were employed in total. The data set was separated into testing and training sets to evaluate the mathematical models created to forecast the loss of wear as a number. The total data, there were 165 samples in the training set (75 %) and 55 samples in the test set (25 %), data during training and testing was assigned at random. To provide accurate comparisons between the three distinct approaches, the same training and test datasets were employed.

3.1. R-Squared (R^2)

R^2 Offers a gauge of how well the model replicates the observed findings depending on the total rate of variance of the outcomes of the framework described in Equation (4).

$$R^2 = 1 - \left[\frac{\sum_i (s_i - p_i)^2}{\sum_i (s_i - \bar{s})^2} \right] \quad (4)$$

3.2. Mean Absolute Error (MAE)

This measure indicates the overall degree of agreement in real units between the predicted and observed datasets. For a perfect model, the outcome is zero and Equation (5) displays a

non-negative observation with no upper bound.

$$MAE = \frac{1}{M} \sum_{j=1}^M |z_j - \bar{e}_j| \quad (5)$$

3.3. Root Mean Square Error (RMSE)

Measuring the variations between actual and expected values in machine learning models is a common application of this technique. The root average square error is the higher degree square of the differences among the actual and expected values, or RMSE shown in Equation (6).

$$RMSE = \frac{1}{M} \times \sum_i |s_i - \theta_i|^2 \quad (6)$$

Fig 1 displays the comparison of experimental and predicted results for the test data and the expected amount of wear loss as well as the range of errors that exist between intended and real forecasts.

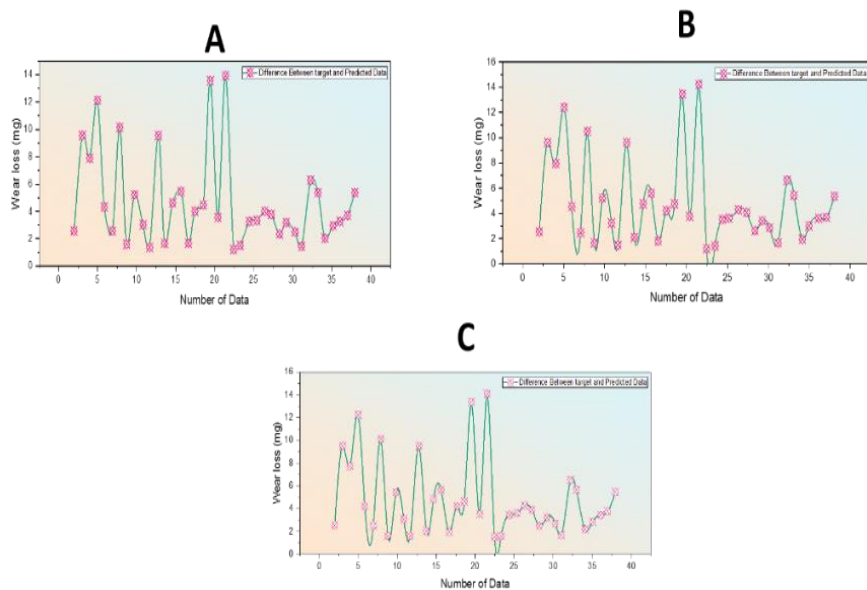


Fig. 1. Comparative of wear loss findings from experiments and predictions A) ANN B) ELM C) ASO-RF (Source: Author)

In Fig 1, all of the constructed models are highly accurate in predicting the experimental findings based on the graphs. The test data shows that the ELM algorithm performs the poorest overall for indices 6, 20 and 34, while the ASO-RF algorithm performs best overall and forecasts wear amount values that are closer to the goal values. The above indices have target values of 6.26, 14.56 and 6.70, respectively. The ELM algorithm predicts values of 6.57, 10.81 and 6.33, in that order. The ASO-RF algorithm has predicted values of 6.69, 11.78 and 6.81, in that order. Fig 2 illustrates error rate of the existing and proposed method.

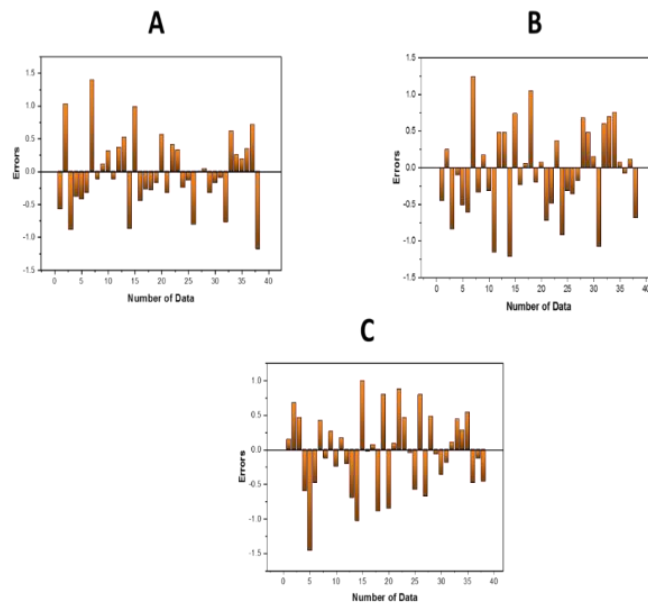


Fig. 2. Error rate models developed with A) ANN, B) ELM, C) ASO-RF (Source: Author)

A detailed evaluation of each model's prediction values' error values can be found in Fig 2. The ASO-RF model's forecast in figure yields the lowest error values. When the model absolute error totals divided by the amount of instances yielded the MAE values, they were compared, For the ANN model, the MAE was determined to be 0.4428, ELM model have the 0.4797, For the ASO-RF model and the optimal MAE value of 0.4369 was calculated. Fig 3 shows the (A-C) Scatter plot of models.

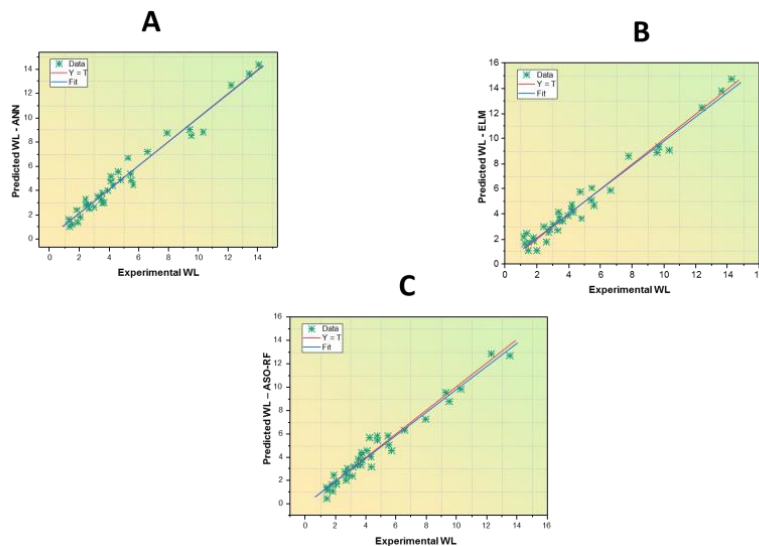


Fig.3. Scatterplot of A) ANN B) ELM C) ASO-RF (Source: Author)

We used scatter plots to show how accurate the models were during the testing periods. R^2 , MAE and RMSE values were evaluated separately for every model to evaluate each of their individual performances. Table 6 shows the parameters for ANN, ELM and ASO-RF. The shortest RMSE value for ASO-RF was found to be 0.5516. The ASO-RF model's calculated R^2 of 0.9730 indicates that it performs better than the remaining methods. Compared to that of ANN, the RMSE measurement for ASO-RF is less than that of ELM and ANN. Considering an MAE value of 0.4370, the ASO-RF approach had the shortest value. The ELM method performed lowest in terms of MAE, while the proposed technique provided a result that was lower than that of the ELM algorithm.

Table 6. An assessment of the specified models' performance (Source: Author)

Model	RMSE	MAE	R^2
Artificial Neural Network (ANN)	0.5526	0.4429	0.9729
Extreme Learning Machine (ELM)	0.5902	0.4798	0.9691
Adaptive Seagull Optimization Integrated Random Forest (ASO-RF)	0.5516	0.4370	0.9730

Our proposed method outperforms other methods in every parameter. It demonstrates superior performance across all evaluated metrics.

4. CONCLUSION

The protective coatings are essential for improving the longevity and performance of magnesium (Mg) alloys in a variety of industrial environments. The present research proposed a unique integrated random forest method for adaptive seagull optimization (ASO-RF) to forecast attrition loss in magnesium alloys coated with spray-on coatings. It demonstrated to generate precise attrition loss projections under a variety of conditions by utilizing wear loss data from AZ91D Mg-alloyed specimens that were exposed to different spray parameters. The AZ91D Mg-alloyed specimens are the specific subject of the study. The proposed method achieved R^2 (0.9730), MAE (0.4370) and RMSE (0.5516). Our proposed method outperforms other methods in every parameter. It demonstrates superior performance across the evaluated metrics. Furthermore, additional validation can be necessary for the suggested method's adaptation to different industrial conditions and magnesium-based composition. It is important to recognize that complicated operating situations and real-world unpredictability can provide obstacles to the method's general adoption. Further research could expand the scope of the suggested approach to encompass various magnesium alloy composition and coat products, investigating its scalability.

References

1. T. Gurgenc, O. Altay, M. Ulas, and C. Ozel, Extreme learning machine and support vector regression wear loss predictions for magnesium alloys coated using various spray coating methods. *Journal of Applied Physics*, vol. 127, no. 18, 2020, DOI: 10.1063/5.0004562
2. F. Aydin, & R. Durgut, Estimation of wear performance of AZ91 alloy under dry sliding conditions using machine learning methods. *Transactions of Nonferrous Metals Society of China*, vol. 31, no. 1, p. 125-137, 2021, DOI: 10.1016/S1003-6326(20)65482-6
3. H. Wu, Y. Zhang, S. Long, L. Zhang, and X. Jie. Tribological behavior of graphene anchored Mg-Al layered double hydroxide film on Mg alloy pre-sprayed Al coating. *Applied Surface Science*, vol. 530, p.146536, 2020, DOI: 10.1016/j.apsusc.2020.146536
4. M. Vardhanapu, P.K. Chaganti, and P. Tarigopula, Characterization and machine learning-based parameter estimation in MQL machining of a superalloy for developed green nano-metalworking fluids. *Journal of the Brazilian Society of Mechanical Sciences and Engineering*, vol. 45 no. 3, p.154, 2023, DOI: 10.1007/s40430-023-04078-0
5. K. Aoudia, D. Retraint, C. Verdy, C. Langlade, J. Creus, and F. Sanchette, Enhancement of Mechanical Properties and Corrosion Resistance of HVOF-Sprayed NiCrBSi Coatings Through Mechanical Attrition Treatment (SMAT). *Journal of Thermal Spray Technology*, vol. 29, pp.2065-2079 2020, DOI: 10.1007/s11666-020-01092-9
6. M. Uddin, C. Hall, V. Santos, R. Visalakshan, G. Qian, and K. Vasilev, Synergistic effect of deep ball burnishing and HA coating on surface integrity, corrosion and immune response of biodegradable AZ31B Mg alloys. *Materials Science and Engineering*: vol. 118, p.111459, 2021, DOI: 10.1016/j.msec.2020.111459
7. R. Nikbakht, S.H. Seyedein, S. Kheirandish, H. Assadi, and B. Jodoin, The role of deposition sequence in cold spraying of dissimilar materials. *Surface and Coatings Technology*, vol. 367, pp.75-85, 2019, DOI: 10.1016/j.surfcoat.2019.03.065
8. R. Kohli, Applications of solid carbon dioxide (dry ice) pellet blasting for removal of surface contaminants. In *Developments in surface contamination and cleaning: applications of cleaning techniques*. Elsevier, pp. 117-169, 2019, DOI: 10.1016/B978-0-12-815577-6.00004-9
9. H. Liu, Z. Tong, Y. Yang, W. Zhou, J. Chen, X. Pan, and X. Ren, Preparation of phosphate conversion coating on laser surface textured surface to improve corrosion performance of magnesium alloy. *Journal of Alloys and Compounds*, vol. 865, p.158701, 2021, DOI: 10.1016/j.jallcom.2021.158701.
10. N. Singh, U. Batra, K. Kumar, N. Ahuja, and A. Mahapatro, Progress in bioactive surface coatings on biodegradable Mg alloys: A critical review towards clinical translation. *Bioactive Materials*, vol. 19, pp.717-757, 2023, DOI: 10.1016/j.bioactmat.2022.05.009
11. V.G. Shmorgun, A.I. Bogdanov, V.P. Kulevich, L.D. Iskhakova, and A.O. Taube, Microstructure and phase composition of diffusion coating formed in NiCr alloys by hot-dip aluminizing. *Surfaces and Interfaces*, vol. 23, p.100988, 2021, DOI: 10.1016/j.surfin.2021.100988
12. T. Gurgenc, O. Altay, M. Ulas, and C. Ozel, Extreme learning machine and support vector regression wear loss predictions for magnesium alloys coated using various spray coating methods. *Journal of Applied Physics*, vol. 127 no. 18, 2020, DOI: 10.1063/5.0004562
13. S.H. Kruthiventi, and D.K. Ammisetti, Experimental Investigation and Machine Learning Modeling of Wear Characteristics of AZ91 Composites. *Journal of Tribology*, vol. 145 no. 10, p.101704 2023, DOI: 10.1115/1.4062518
14. T. Gurgenc, Microstructure, mechanical properties and ELM based wear loss prediction of plasma sprayed ZrO₂-MgO coatings on a magnesium alloy. *Materials Testing*, vol. 61 no. 8, pp.787-796, 2019, DOI: 10.3139/120.111387
15. P. Hulipalled, V. Algur, V. Lokesha, and S. Saumya, Interpretable ensemble machine learning framework to predict wear rate of modified ZA-27 alloy. *Tribology International*, vol. 188,

- p.108783, 2023, DOI: 10.1016/j.triboint.2023.108783
- 16. S.V. Alagarsamy, R. Balasundaram, M. Ravichandran, V. Mohanavel, A. Karthick, and S.S. Devi, Taguchi approach and decision tree algorithm for prediction of wear rate in zinc oxide-filled AA7075 matrix composites. *Surface Topography: Metrology and Properties*, vol. 9 no. 3, p.035005, 2021, DOI: 10.1088/2051-672X/ac0f34
 - 17. A. Moses, D. Chen, P. Wan, and S. Wang, Prediction of electrochemical corrosion behavior of magnesium alloy using machine learning methods. *Materials Today Communications*, vol. 37, p.107285, 2023, DOI: 10.1016/j.mtcomm.2023.107285
 - 18. F. König, C. Sous, A.O. Chaib, and G. Jacobs, Machine learning-based anomaly detection and classification of acoustic emission events for wear monitoring in sliding bearing systems. *Tribology International*, vol. 155, p.106811, 2021, DOI: 10.1016/j.triboint.2020.106811
 - 19. A.A. Deliwala, K. Dubey, and C.S. Yerramalli, Predicting the Erosion Rate of Uni-Directional Glass Fiber Reinforced Polymer Composites Using Machine-Learning Algorithms. *Journal of Tribology*, vol. 144 no. 9, p.091707, 2022, DOI: 10.1115/1.4054247
 - 20. H. Zhao, Effect Of Magnesium Alloy Surface Spray Coating On The Wear Resistance Of Sports Equipment. *Journal of Applied Science and Engineering*, vol. 26 no. 3, pp.423-432, 2022,
 - 21. M. Ulas, O. Altay, T. Gurgenc, and C. Özal, A new approach for prediction of the wear loss of PTA surface coatings using artificial neural network and basic, kernel-based, and weighted extreme learning machine. *Friction*, vol. 8, pp.1102-1116, 2020, DOI: 10.1007/s40544-017-0340-0